CHINESE OPTICS LETTERS

Vol. 22, No. 5 | May 2024

Mid-infrared SESAM mode-locked Er:CaF_2-SrF_2 bulk laser at 2.73 μm

Jingjing Liu (刘晶晶)[1], Linxuan Tang (唐琳萱)[1], Xiaoyue Feng (冯潇玥)[1], Mengyu Zong (宗梦雨)[1], Luyang Tong (仝鲁阳)[1], Zhen Zhang (张 振)[2,3], Lina Zhao (赵丽娜)[1], Jie Liu (刘 杰)[1*], and Liangbi Su (苏良碧)[2,3**]

[1] Shandong Provincial Engineering and Technical Center of Light Manipulations and Shandong Provincial Key Laboratory of Optics and Photonic Device, School of Physics and Electronics, Shandong Normal University, Jinan 250358, China

[2] CAS Key Laboratory of Transparent and Opto-Functional Inorganic Materials, Synthetic Single Crystal Research Center, Shanghai Institute of Ceramics, Chinese Academy of Sciences, Shanghai 201899, China

[3] State Key Laboratory of High Performance Ceramics and Superfine Microstructure, Shanghai Institute of Ceramics, Chinese Academy of Sciences, Shanghai 201899, China

*Corresponding author: jieliu@sdnu.edu.cn

**Corresponding author: suliangbi@mail.sic.ac.cn

Received January 18, 2024 | Accepted February 5, 2024 | Posted Online May 17, 2024

To the best of our knowledge, this is the first time that a mid-infrared Er^{3+}:CaF_2-SrF_2 laser has achieved continuous-wave mode-locked operation by a semiconductor saturable absorber mirror. The laser emits a maximum output power of 93 mW at 2.73 μm with a repetition rate of approximately 69 MHz and demonstrates a high signal-to-noise ratio of around 71 dB. In addition, a MgF_2 birefringent plate was utilized to enable wavelength tuning of the Er^{3+}:CaF_2-SrF_2 laser, resulting in operation at approximately 2.73 μm, 2.75 μm, 2.79 μm, and 2.81 μm. These results demonstrate that Er^{3+}:CaF_2-SrF_2 is a promising alternative for the generation of efficient diode-pumped mode-locked lasers around 2.8 μm.

Keywords: mid-infrared laser; mode-locked laser; tunable wavelength.
DOI: 10.3788/COL202422.051406

1. Introduction

Mid-infrared ultrafast laser sources exhibit a distinctive output wavelength and extremely narrow pulse duration (picosecond to femtosecond level), leading to many significant applications[1,2]. As well-known, the 2–5 μm spectral range in the mid-infrared region covers numerous absorption peaks of many atoms and molecules, also referred to as the molecular fingerprint region[3,4]. It is worth noting that water molecules tend to exhibit a significant absorption peak, especially around 3 μm. Therefore, the 3 μm ultrafast laser has a unique application in laser surgery, often referred to as the "golden scalpel" for its precision[5]. Additionally, mid-infrared 3 μm mode-locked lasers can be employed for optical frequency comb generation[6], serving as pump sources for mid-infrared supercontinuum light[7]. These mid-infrared light sources find crucial applications in molecular spectroscopy, remote sensing, optical communication, and other related fields.

In the past, mid-infrared ultrafast laser sources were mainly produced by the optical parametric oscillator (OPO) and quantum cascade laser[8–10], which has many problems such as generally high price, complex construction, and low conversion efficiency. In recent years, the mode-locked fluoride fiber laser has emerged as a simple and economic way to directly generate ultrashort pulses in the mid-infrared range[11–15]. Despite the flexible output, compact structure, and high beam quality of the mid-infrared fiber laser utilizing soft glass fiber, there remain several unresolved issues, including poor mechanical strength, low softening point of glass, and susceptibility to deliquescence[16]. The stability of the rare-earth-ion-doped mid-infrared solid-state laser has garnered significant attention from researchers, as it enables high power laser output and facilitates ultrafast laser applications[17–21].

Er^{3+} and Ho^{3+} are the commonly used rare-earth ions employed as the active ions in the 3 μm solid-state laser. In the latest development, researchers have reported the operations of solid-state lasers with *Q*-switched mode-locking at a wavelength of 3 μm. In 2018, our team successfully utilized a semiconductor saturable absorber mirror (SESAM) to achieve a 2.7 μm *Q*-switched mode-locked laser in Er:CaF_2-SrF_2 crystal, marking a significant result with the pulse duration of the mode-locked sequence on the order of nanoseconds[22]. In the same year, Xue *et al.* reported a stable *Q*-switched mode-locked 2.7 μm Er:Y_2O_3 ceramic laser by using a SESAM, and the pulse duration of the mode-locked sequence was less than 1.43 ns[23]. In their study, Yang *et al.* utilized a SESAM to generate

Q-switched mode-locked pulse laser output in a Ho, Pr :$LiLuF_4$ medium. The mode-locked sequence exhibited a pulse duration of approximately 640 ps[24]. In 2019, Svejkar and colleagues were able to achieve passive Q-switched mode-locking in an Er:Y_2O_3 crystal, resulting in mode-locked sequences with pulse durations of about 86 ps[25]. To our understanding, there have not been any reports regarding the operation of a continuous wave mode-locked (CWML) laser for a diode-pumped mid-infrared 3 μm solid-state laser using Er^{3+}-doped or Ho^{3+}-doped crystals. In addition, CaF_2 and SrF_2 crystals have a fluorite structure, which is used in this study and is known for its ease of growth to a large size, providing convenience for industrialization.

In this study, we have successfully shown the first demonstration of a passive CWML laser using a compact W-type cavity, based on the Er^{3+}:CaF_2-SrF_2 crystal. The CWML laser reached a maximum power of 93 mW, while maintaining a repetition rate of 69.03 MHz and achieving a high signal-to-noise ratio of approximately 71 dB. Besides, the wavelength-tunable laser emitting around 2.8 μm was obtained by using a MgF_2 birefringent plate (BF).

2. Experiments

In this experiment, a commercial fiber-coupled single-tube laser diode (LD) emitting a wavelength locked at 976 nm was used as the pumping source. The LD had a core diameter of approximately 105 μm and a numerical aperture (NA) of 0.15. A 1:2 compression ratio coupling system was used to inject the pump laser into the gain medium, and a W-type folded cavity was used for this experiment in Fig. 1. The laser power and waveform can be monitored simultaneously with two output beams output behind the output coupler (OC). The input mirror (IM) is a flat mirror that has a high-reflection (HR) coating for 2.7–2.95 μm and an anti-reflection (AR) coating for 970–980 nm. The M2 and M3 folding mirrors are set at an angle with curvature radii of 200 mm and 100 mm, respectively. Both mirrors were coated with HR material for wavelengths between 2.7 and 2.95 μm. The OC has a transmission of 1% at 2.7–2.95 μm and a curvature radius of 500 mm. The mirror M4, which has an HR coating for 2.7–2.95 μm, has been configured for continuous wave (CW) laser operation. Likewise, the SESAM has also been configured for CWML laser operation. The gain medium was an uncoated Er^{3+}:$Ca_{0.8}Sr_{0.2}F_2$ crystal with an Er^{3+} doping concentration of 3.0% (atomic fraction). The crystal was carefully placed in a copper block that was maintained at a stable temperature of 12°C through the use of circulating cooling water. Additionally, both ends of the crystal were expertly polished, and it had precise dimensions of 3 mm × 3 mm × 10 mm. It is also important to mention that the laboratory maintains a humidity level of approximately 12%. The laser mode radius of the laser crystal in the W-type cavity is about 110 μm, while the laser mode radius on the SESAM was estimated to be about 35 μm using the ABCD matrix transformation theory. Additionally, the length of the W-type resonator was measured to be roughly 2.17 m.

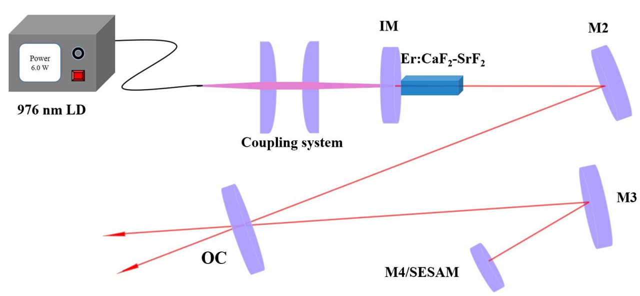

Fig. 1. Schematic setup of the mode-locked Er:CaF_2-SrF_2 laser at 2.73 μm.

3. Results and Discussion

For the laser tuning operation, we selected a V-type resonant cavity. The pumping source, IM, and the fold mirror M2 are the same as Fig. 1. There is an additional plane mirror, labeled as OC, which has a transmission of 3% for wavelengths between 2.7 and 2.95 μm. A MgF_2 BF was positioned at the Brewster angle within the cavity, and it had a thickness of 1 mm. At an incident pump power of 2.5 W, by rotating the MgF_2 BF, a wavelength-tunable Er^{3+}:CaF_2-SrF_2 laser was operated discontinuously among 2.73 μm, 2.75 μm, 2.79 μm, and 2.81 μm. The separated tuning wavelengths were shown in Fig. 2. Xu *et al.* also realized the operation of the tunable laser in Er:Y_2O_3 ceramic, and the obtained tuned spectral lines are also discontinuous[19].

In Fig. 3, we can see the dependency of the average output power on the absorbed pump power for both CW and passively mode-locked operation. The CW laser output characteristics have been investigated with a plane reflecting mirror (M4) instead of a SESAM. For the CW laser operation, the maximum output power was 304 mW, while the slope efficiency was approximately 11.5%. By precisely adjusting the cavity mirrors and ensuring the absorbed pump power exceeds 1.92 W, the SESAM (BATOP GmbH, SAM-2400-1-10ps) enabled the laser to operate in the CWML mode. The maximum output power of 93 mW in the CWML mode was obtained, while the slope efficiency was approximately 3.6%.

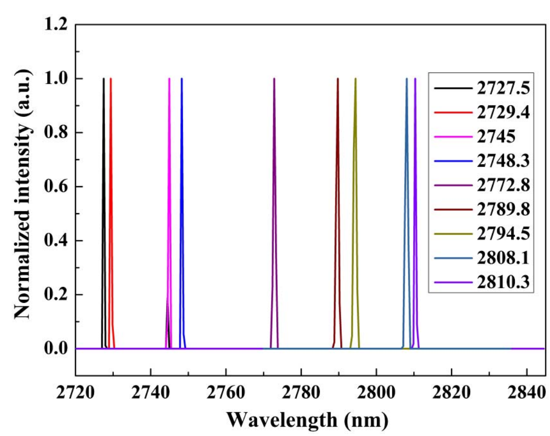

Fig. 2. Tunable wavelength of Er:CaF_2-SrF_2 laser.

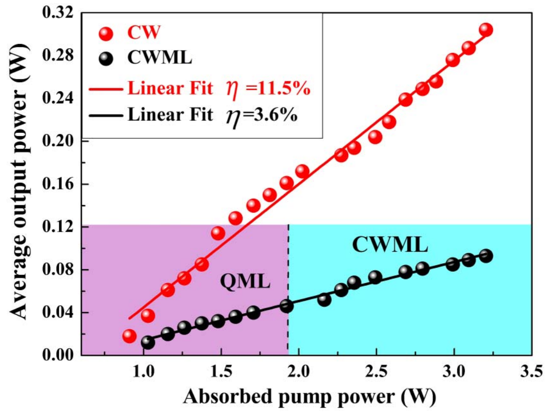

Fig. 3. For the W-type resonator, average output powers versus absorbed pump powers for both CW and passively CWML laser operation.

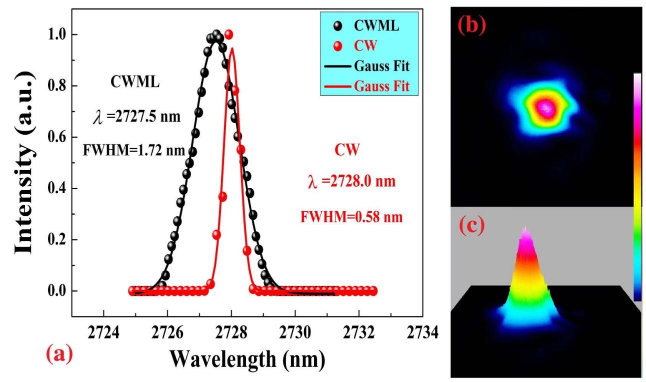

Fig. 6. (a) Spectra of the Er:CaF_2-SrF_2 lasers in the CW and CWML regime; (b) laser beam profile; (C) 3D light intensity distribution recorded for the CWML laser operation.

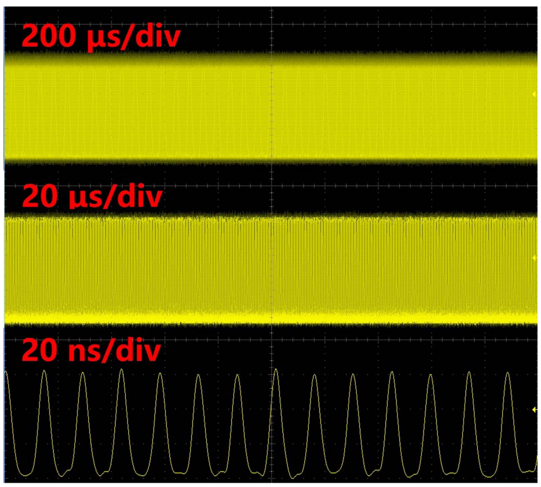

Fig. 4. Oscilloscope recorded typical CWML pulse trains for various time scales.

Figure 4 displays the mode-locked pulse sequences captured at various time scales through the utilization of a Tektronix DPO4104 digital oscilloscope. The oscilloscope was connected to a mid-infrared HgCdTe photodetector to obtain the pulse optical signal. Additionally, the radio frequency (RF) spectra in Fig. 5 were recorded using a Rohde & Schwarz-FSC spectrum analyzer with different sweep ranges. Figure 5(a) presents a signal-to-noise ratio of ~71 dB with the sweep range of 67.5–71 MHz at a resolution bandwidth (RBW) of 1 kHz. Figure 5(b) presents higher order harmonic signal with the sweep range of 0–500 MHz at an RBW of 30 kHz.

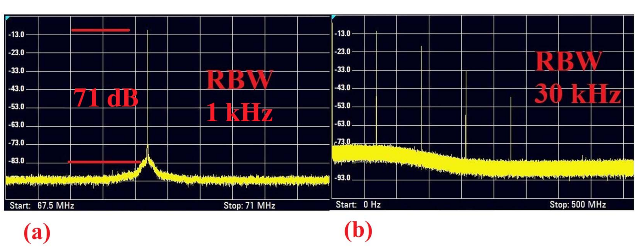

Fig. 5. The RF spectra of the CWML laser were recorded for different sweep ranges.

As can be seen from the Fig. 6(a), the laser emission spectra for CW and CWML mode were recorded by an optical spectrum analyzer (SOL-MS3504i). The CW laser has a central wavelength of 2728.0 nm and an FWHM of about 0.58 nm. For the CWML mode, the central wavelength of 2727.5 nm obtained an FWHM of approximately 1.72 nm, using the Gaussian fit. Based on the spectrum and its spectral width, we can make an estimate of the pulse width. The theoretical pulse width $\Delta\tau$ was determined by the following equations:

$$\Delta\nu = \frac{c}{\lambda^2}\Delta\lambda, \tag{1}$$

$$\Delta\nu \times \Delta\tau = 0.4412, \tag{2}$$

where $\Delta\lambda$ was the linewidth of the CWML laser emission spectrum. The minimum pulse width can be calculated to be about 6.4 ps in theory, so the actual pulse duration was on the order of 10 ps. However, due to the CWML laser with two output beams, the single beam power is too low to measure the actual pulse duration by the commercial autocorrelation instrument. With the limitation of SESAM wavelength, we only achieve mode-locking at 2.73 μm at the short wavelength of the tuning laser. Long-band mode-locking can be achieved in the near future with an optimized SESAM. Figures 6(b) and 6(c) display the laser beam profile and light intensity distribution, respectively, which were recorded by a detector. The results indicated that the generated beam had an excellent TEM_{00} transversal profile.

4. Conclusion

In conclusion, it can be stated that a mid-infrared Er^{3+}:CaF_2-SrF_2 laser has been successfully operated at 2727.5 nm in CWML operation using a SESAM. The maximum output power reached 93 mW, while the repetition rate was

69.03 MHz. The CWML laser also has a high signal-to-noise ratio of approximately 71 dB. Using a MgF_2 BF, a wavelength-tunable laser emitting around 2.8 μm was obtained based on this crystal. These results indicated that Er^{3+}:CaF_2-SrF_2 crystal is promising for the generation of ultrashort pulse lasers in the mid-infrared region.

Acknowledgements

This work was supported by the National Natural Science Foundation of China (Nos. 12374401, 12104271, and 61925508), the Natural Science Foundation of Shandong Province (Nos. ZR2021LLZ008 and ZR2021QA030), and the China Postdoctoral Science Foundation (No. 2021M691981).

References

1. R. Won, "Shining in the mid-infrared," Nat. Photonics **5**, 457 (2011).
2. R. I. Woodward, D. D. Hudson, A. Fuerbach, *et al.*, "Generation of 70-fs pulses at 2.86 μm from a mid-infrared fiber laser," Opt. Lett. **42**, 4893 (2017).
3. H. Timmers, A. Kowligy, A. Lind, *et al.*, "Molecular fingerprinting with bright, broadband infrared frequency combs," Optica **5**, 727 (2018).
4. A. Schliesser, N. Picque, and T. W. Hansch, "Mid-infrared frequency combs," Nat. Photonics **6**, 440 (2012).
5. J. T. Walsh, T. J. Flotte, and T. F. Deutsch, "Er:YAG laser ablation of tissue: effect of pulse duration and tissue type on thermal damage," Lasers Surg. Med. **9**, 314 (1989).
6. A. Hugi, G. Villares, S. Blaser, *et al.*, "Mid-infrared frequency comb based on a quantum cascade laser," Nature **492**, 229 (2012).
7. D. D. Hudson, S. Antipov, L. Li, *et al*, "Toward all-fiber supercontinuum spanning the mid-infrared," Optica **4**, 1163 (2017).
8. H. T. Huang, S. Q. Wang, X. Liu, *et al.*, "Simultaneous dual-wavelength nanosecond mid-infrared optical parametric oscillator," Infrared Phys. Technol. **93**, 91 (2018).
9. K. Chen, D. G. Xu, J. N. Li, *et al.*, "Widely independent tunable dual-color mid-infrared optical parametric oscillator based on $BaGa_4Se_7$ crystals," Opt. Laser Technol. **167**, 109750 (2023).
10. X. Yang, Z. R. Zhang, S. Yang, *et al.*, "Development of a rapid measurement method for analysis of the NOx conversion process based on quantum cascade laser absorption spectroscopy," Sensors **23**, 3885 (2023).
11. S. Duval, M. Bernier, V. Fortin, *et al.*, "Femtosecond fiber lasers reach the mid-infrared," Optica **2**, 623 (2015).
12. Z. P. Qin, G. Q. Xie, J. G. Ma, *et al.*, "2.8 μm all-fiber *Q*-switched and mode-locked lasers with black phosphorus," Photonics Res. **6**, 1074 (2018).
13. G. L. Li, C. Y. Ma, J. Peng, *et al.*, "Modelling the sub-100 fs Dy^{3+}: fluoride fiber laser beyond 3 μm," Opt. Laser Technol. **158**, 108861 (2023).
14. Z. P. Qin, G. Q. Xie, H. A. Gu, *et al.*, "Mode-locked 2.8-μm fluoride fiber laser: from soliton to breathing pulse," Adv. Photonics **1**, 065001 (2019).
15. H. Y. Luo, J. Yang, J. F. Li, *et al.*, "Tunable sub-300 fs soliton and switchable dual-wavelength pulse generation from a mode-locked fiber oscillator around 2.8 μm," Opt. Lett. **46**, 841 (2021).
16. S. C. Ruan, J. Hou, J. F. Li, *et al.*, "The introduction of special issue on technology and application of advanced mid-infrared lasers," Chin. J. Lasers **49**, 0101000 (2022).
17. Y. Y. Liang, T. Li, B. T. Zhang, *et al.*, "14.1 W continuous-wave dual-end diode-pumped Er:Lu_2O_3 laser at 2.85 μm," Chin. Opt. Lett. **22**, 011403 (2024).
18. Y. P. Yao, N. Cui, Q. G. Wang, *et al.*, "Highly efficient continuous-wave and $ReSe_2$ *Q*-switched ∼3 μm dual-wavelength Er:YAP crystal lasers," Opt. Lett. **44**, 2839 (2019).
19. X. F. Guan, J. W. Wang, Y. Z. Zhang, *et al.*, "Self-*Q*-switched and wavelength-tunable tungsten disulfide-based passively *Q*-switched Er:Y_2O_3 ceramic lasers," Photonics Res. **6**, 830 (2018).
20. Z. Q. Fang, D. L. Sun, J. Q. Luo, *et al.*, "A modified formula of thermal focal length for lamp pumping Cr, Er:YSGG crystal with high performance 2.79 μm laser," Opt. Laser Technol. **115**, 398 (2019).
21. W. C. Yao, H. Uehara, H. Kawase, *et al.*, "Highly efficient Er:YAP laser with 6.9 W of output power at 2920 nm," Opt. Express **28**, 19000 (2020).
22. J. J. Liu, X. Feng, X. Fan, *et al.*, "Efficient continuous-wave and passive *Q*-switched mode-locked Er^{3+}:CaF_2-SrF_2 lasers in the mid-infrared region," Opt. Lett. **43**, 2418 (2018).
23. H. Xue, L. Wang, W. Zhou, *et al.*, "Stable *Q*-switched mode-locking of 2.7 μm Er:Y_2O_3 ceramic laser using a semiconductor saturable absorber," Appl. Sci. **8**, 1155 (2018).
24. Y. Yang, H. Nie, B. Zhang, *et al.*, "Passively *Q*-switched mode-locked Ho, Pr:$LiLuF_4$ laser operating at 2.9 μm with semiconductor saturable absorber mirror," Appl. Phys. Express **11**, 112704 (2018).
25. R. Švejkar, J. Šulc, and H. Jelínková, "Er:Y_2O_3 high-repetition rate picosecond 2.7 μm laser," Laser Phys. Lett. **16**, 075802 (2019).